*Desalination and Water Treatment*
www.deswater.com
doi: 10.1080/19443994.2014.904823

54 (2015) 2883–2890
May

Taylor & Francis
Taylor & Francis Group

# Ion-exchange kinetic studies for Cd(II), Co(II), Cu(II), and Pb(II) metal ions over a composite cation exchanger

Mu. Naushad[a,*], Alok Mittal[b], M. Rathore[c], V. Gupta[d]

[a]*Department of Chemistry, College of Science, King Saud University, Building #5, Riyadh, Kingdom of Saudi Arabia, Tel. +966 14674198; email: shad81@rediffmail.com*
[b]*Department of Chemistry, Maulana Azad National Institute of Technology, Bhopal, India*
[c]*Department of Chemistry, Sri Venktateshwara University, Gajraula, India*
[d]*Department of Chemistry, IFTM University, Moradabad, India*

Received 28 January 2014; Accepted 5 March 2014

ABSTRACT

Explicit Nernst–Planck approximation is used to study the kinetics of H(I)-metal ion-exchange processes for ions having different effective diffusion coefficients, that is, for non-isotopic exchange process. Kinetic studies of four heavy metal ions ($Cd^{2+}$, $Co^{2+}$, $Cu^{2+}$, and $Pb^{2+}$) of environmental importance on the surface of acetonitrile stannic(IV) selenite composite cation exchanger were carried out successfully. On the basis of kinetic studies, various physical parameters, that is, fractional attainment of equilibrium $U(\tau)$, self-diffusion coefficients ($D_o$), energy of activation ($E_a$), and entropy of activation ($\Delta S^*$) are estimated to evaluate the mechanism of ion exchange on the surface of composite ion-exchange material. The activation entropy and energy revealed that the greater degree and minimum energy was achieved during forward ion-exchange process. The results revealed that the kinetic studies are very important for the economic and industrial applications of ion-exchange materials.

*Keywords:* Acetonitrile stannic(IV) selenite; Cation exchanger; Ion-exchange kinetics

## 1. Introduction

The presence of pesticides, radionuclides, and most importantly heavy toxic metal ions in the aquatic environment has been of great concern to engineers, environmentalists, and scientists because of their increased discharge, toxic nature, and adverse effects on the receiving water. Among the toxic metal species, $Cd^{2+}$, $Co^{2+}$, $Cu^{2+}$, and $Pb^{2+}$ are on the priority list of various Environmental Protection Agencies worldwide [1–3]. The existence of these toxic metal species in the aquatic environment through naturally or human anthropogenic sources may cause several health hazards including gastrointestinal distress, liver and kidney damage, Alzheimer's and Parkinson's diseases, carcinogenic, vasodilation, flushing, and cardiomyopathy, blood pressure, paralysis, diarrhea, lung irritation and bone defects, pernicious anemia in humans and animals [4,5]. This is well thought out due the non-biodegradable nature, high solubility, and easy to enter into human as well animal body through food chains. It is well understood that heavy metal ions are toxic to the environment even at very low concentration levels [6]. The adverse effects of heavy toxic metal ions on environment counsel that the wastewater should be treated before discharging to the public

*Corresponding author.

sewage, rivers, or on lands, etc. Several technologies including thermal treatment, surface-enhanced Raman spectrometry, inductively coupled plasma mass spectrometry, inductively coupled plasma optical emission spectrometry, precipitation, atomic absorption spectrometry (AAS), ion chromatography, flame AAS, extraction, square wave anodic stripping voltammetry, adsorption, UV–vis spectrometry, atomic fluorescence spectrometry, colorimetric analysis, and ion exchange have been proposed for the removal of these pollutants from the aquatic environment [7–23]. Among these techniques, ion exchange is one of the most common and effective treatment methods. Ion-exchange method may have the various advantages such as regeneration capability of ion-exchange materials, low cost, pH independence, high selectivity, etc. Various types of ion-exchange materials including inorganic, organic, and composite ion-exchange materials are being used for the wastewater treatment worldwide [24–29]. Nowadays, organic–inorganic-type composite ion-exchange materials, inorganic and organic ion-exchange materials are being extensively used for wastewater treatment without studying the validity of ion-exchange mechanism [30–32]. Thus, our group is actively engaged to study the issues related to the ion-exchange kinetics and the mobility of counter ions in the lattice structure of newly synthesized ion-exchange materials. Therefore, in this research study, acetonitrile stannic(IV) selenite composite cation-exchange material was selected to evaluate the ion-exchange mechanism occurring over the surface of the ion exchanger.

## 2. Experimental

### 2.1. Materials and instruments

The main reagents used for the synthesis of the material were stannic chloride penta-hydrate, sodium selenite, and acetonitrile (Sigma–Aldrich, Saudi Arabia). Solutions for kinetic measurement were made using analytical reagent grade nitrate salts of Cd, Co, Cu, and Pb (99%) (Sigma–Aldrich, Saudi Arabia). Nitric acid (35%) and hydrochloric acid (35%) were also obtained from Sigma–Aldrich, Saudi Arabia. All other reagents and chemicals were of analytical reagent grade. A single electrode pH meter (Orion 2 star, Thermo Scientific, USA) and a water bath incubator shaker (SW22/9550322, Julabo, Germany) were used.

### 2.2. Methods

Composite cation-exchanger acetonitrile stannic(IV) selenite was prepared as reported by Nabi et al. [33]. The procedure for the preparation is given below.

#### 2.2.1. Preparation of acetonitrile stannic(IV) selenite composite cation-exchange material

Inorganic cation exchanger was prepared by mixing gradually with continuous shaking an aqueous solution of 0.1 M sodium selenite into 0.1 M Sn(IV) chloride penta-hydrate solution in (1:2) mixing volume ratio at pH 1.5. To prepare composite cation exchanger, one volume of (10%) acetonitrile was added drop wise into the inorganic precipitate of stannic(IV) selenite and mixed thoroughly with constant stirring for 1 h. The gelatinous precipitate so formed was allowed to stand for 24 h in the mother liquor for digestion. The supernatant liquid was removed and the precipitate was washed with demineralized water several times to remove excess reagents. The product was dried at 40 ± 2°C in an oven. The dried product was then kept in demineralized water for cracking and to obtain the particle of the size range approximately 125 m. These were converted to $H^+$ form by placing them in 1 M $HNO_3$ solution and washed with demineralized water to remove excess acid and finally dried at 45± °C.

#### 2.2.2. Method for the measurement of ion-exchange capacity

The ion-exchange capacity was determined by standard column process. For this purpose, 1 g of the dry cation exchanger in the $H^+$-form was taken into a glass column having an internal diameter (i.d.) ~1 cm and fitted with glass wool support at the bottom. The bed length was approximately 1.5 cm long. 1 M $NaNO_3$ as eluent was used to elute the $H^+$ ions completely from the cation-exchange column, maintaining a very slow flow rate (~0.5 mL $min^{-1}$). The effluent was titrated against a standard 0.1 M NaOH solution for the total ions liberated in the solution using phenolphthalein indicator and the ion-exchange capacity was determined. The ion-exchange capacity of this composite cation exchanger was found to be 1.83 meq $g^{-1}$.

### 2.3. Determination of theoretical approach

Composite cation-exchanger particles of mean radii ~125 μm (50–70 mesh) in $H^+$ form were used to evaluate various kinetic parameters. The rate of exchange was calculated as follows.

A total of 20 mL fractions of the 0.02 M metal ion solutions (Cd, Co, Cu, and Pb) were shaken with 200 mg of the cation exchanger in $H^+$-form in several stoppered conical flasks at desired temperatures [25, 35, 55, and 65 (± 0.5) °C] for different time intervals (1.0,

2.0, 3.0, and 4.0 min). The supernatant liquid was removed immediately and determinations were made as usual by ethylene diamine tetra acetic acid, disodium salt titrations [34]. Each set was repeated four times, and the mean values were taken for calculation.

## 3. Results and discussion

Cation-exchange materials consist essentially fixed positive backbone with negatively charged anionic groups, the electric charge of which is compensated for the mobile ions of opposite charge, that is, counter ions. These counter ions are free to diffuse within the ion-exchange materials. Generally, in an ion-exchange process, the counter ion present initially is replaced by another species. Ion-exchange process takes place stoichiometrically by the effective exchange of counter ions A with the counter ions B present at the surface of ion-exchange materials. In fact, ions A diffuse out of the ion-exchange materials and are replaced by an equivalent amount of B. Simply, the rate determining mechanism is the interdiffusion of the two species A and B either within the ion-exchange material or in a Nernst diffusion layer "film" adherent to the particle surface [35]. Various limiting laws for film-controlled exchange have been given previously. In this study, ideal limiting laws for particle controlled process are determined.

In principle kinetic studies envisage the three aspects of ion-exchange process viz. the mechanism of ion exchange, rate determining step, and the rate laws obeyed by the ion-exchange system. In an ion-exchange process, the interdiffusion of counter ions is occurring either by particle diffusion or film diffusion control. A simple kinetic criterion is used to predict whether particle or film diffusion will be rate controlling step under a given set of conditions. The infinite time of exchange is the time necessary to obtain equilibrium in an ion-exchange process. Thus, the ion-exchange rate becomes independent of time after this time interval. Fig. 1 showed that 25 min was required for the establishment of equilibrium at 25°C for $Mg^{2+}$–$H^+$ exchange. Similar behavior was also observed for $Cd^{2+}$–$H^+$, $Co^{2+}$–$H^+$, $Cu^{2+}$–$H^+$, and $Pb^{2+}$–$H^+$ exchanges. Therefore, 25 min was assumed to be the infinite time of exchange for all exchange systems.

Fig. 2 showed that the $\tau$ vs. time ($t$) ($t$ in min) plots are also straight lines passing through the origin at and above 0.02 M of metal ion concentration confirming the particle diffusion control phenomenon. However, below the metal ion concentration of 0.02 M, film diffusion control phenomenon was more prominent. Therefore, the kinetic studies for exchange of $Cd^{2+}$–$H^+$, $Co^{2+}$–$H^+$, $Cu^{2+}$–$H^+$, and $Pb^{2+}$–$H^+$ were made under particle diffusion controlled phenomenon. The kinetic results are expressed in terms of the fractional attainment of equilibrium, $U(\tau)$ with time according to the equation:

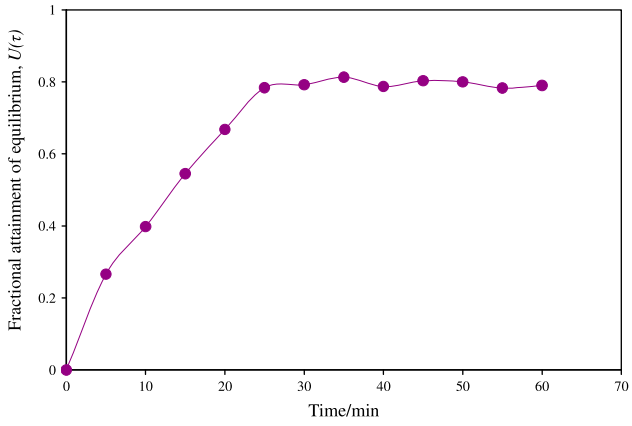


Fig. 1. A plot of $U(\tau)$ vs. $t$ (time) for $M^{2+}$–$H^+$ exchanges at 25°C on acetonitrile stannic(IV) selenite composite cation exchanger for the determination of infinite time.

$$U(\tau) = \frac{\text{the amount of exchange at time } 't'}{\text{the amount of exchange at infinite time}} \quad (1)$$

Fig. 3 shows plots of $U(\tau)$ vs. time ($t$) ($t$ in min) for $Cd^{2+}$–$H^+$, $Co^{2+}$–$H^+$, $Cu^{2+}$–$H^+$, and $Pb^{2+}$–$H^+$ exchanges which indicated that the fractional attainment of equilibrium was faster at a higher temperature suggesting that the mobility of the ions increased with an increase in temperature and the uptake decreased with time.

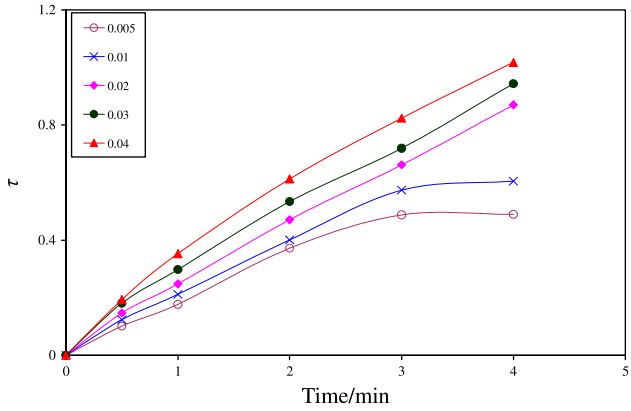


Fig. 2. Plots of $\tau$ vs. $t$ (time) for $M^{2+}$–$H^+$ exchanges using different metal solution concentrations at 25°C on acetonitrile stannic(IV) selenite composite cation exchanger.

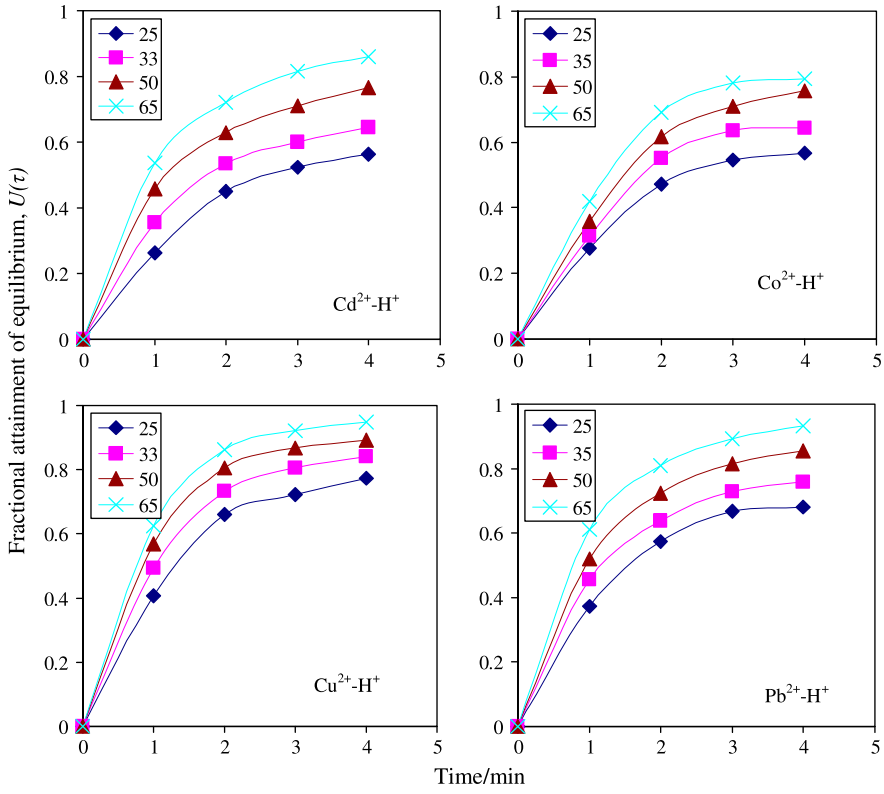


Fig. 3. Plots of $U(\tau)$ vs. $t$ (time) for $Cd^{2+}$–$H^+$, $Co^{2+}$–$H^+$, $Cu^{2+}$–$H^+$, and $Pb^{2+}$–$H^+$ exchanges at different temperatures on acetonitrile stannic(IV) selenite composite cation exchanger.

Each value of $U(\tau)$ will have a corresponding value of $\tau$, a dimensionless time parameter. On the basis of the Nernst–Planck equation, the numerical results can be expressed by explicit approximation [36–38]:

$$U(\tau) = \{1 - \exp[\pi^2(f_1(\alpha)\tau + f_2(\alpha)\tau^2 + f_3(\alpha)\tau^3)]\}^{1/2} \quad (2)$$

where $\tau$ is the half time of exchange = $\overline{D}_{H^+}t/r_o^2$, $\alpha$ is the mobility ratio = $\overline{D}_{H^+}/\overline{D}_{M^{2+}}$, $r_o$ is the particle radius, $\overline{D}_{H^+}$ and $\overline{D}_{M^{2+}}$ are the interdiffusion coefficients of counter ions $H^+$ and $M^{2+}$, respectively, in the exchanger phase. The three functions $f_1(\alpha)$, $f_2(\alpha)$ and $f_3(\alpha)$ depend upon the mobility ratio ($\alpha$) and the charge ratio ($Z_{H^+}/Z_{M^{2+}}$) of the exchanging ions. Thus, they have different expressions as given below [39]. When the exchanger is taken in the $H^+$-form and the exchanging ion is $M^{2+}$, for $1 \le \alpha \le 20$, as in the present case, the three functions have the values.

$$f_1(\alpha) = -\frac{1}{0.64 + 0.36\,\alpha^{0.668}}$$

$$f_2(\alpha) = -\frac{1}{0.96 - 2.0\,\alpha^{0.4635}}$$

$$f_3(\alpha) = -\frac{1}{0.27 + 0.09\,\alpha^{1.140}}$$

The Nernst–Planck explicit approximation Eq. (2) was used to calculate various $\tau$ values corresponding to each $U(\tau)$ using a computer. Fig. 4 showed the plots of $\tau$ vs. time ($t$) at four different temperatures for heavy metal ion-hydrogen exchanges. The straight lines passing through the origin confirming the particle diffusion control phenomenon for $M^{2+}$–$H^+$ exchange at a metal ion concentration of 0.02 M.

The slopes ($S$ values) of various $\tau$ vs. time ($t$) plots are given in Table 1. The $S$ values are related to $\overline{D}_{H^+}$ as follows:

$$S = \overline{D}_{H^+}/r_0^2 \quad (3)$$

The values of $-\log \overline{D}_{H^+}$ obtained by using Eq. (3) plotted against $1/T$ are straight lines as shown in Fig. 4, thus verifying the validity of the Arrhenius relation:

$$\overline{D}_{H^+} = D_0 \exp(-E_a/\mathrm{RT}) \quad (4)$$

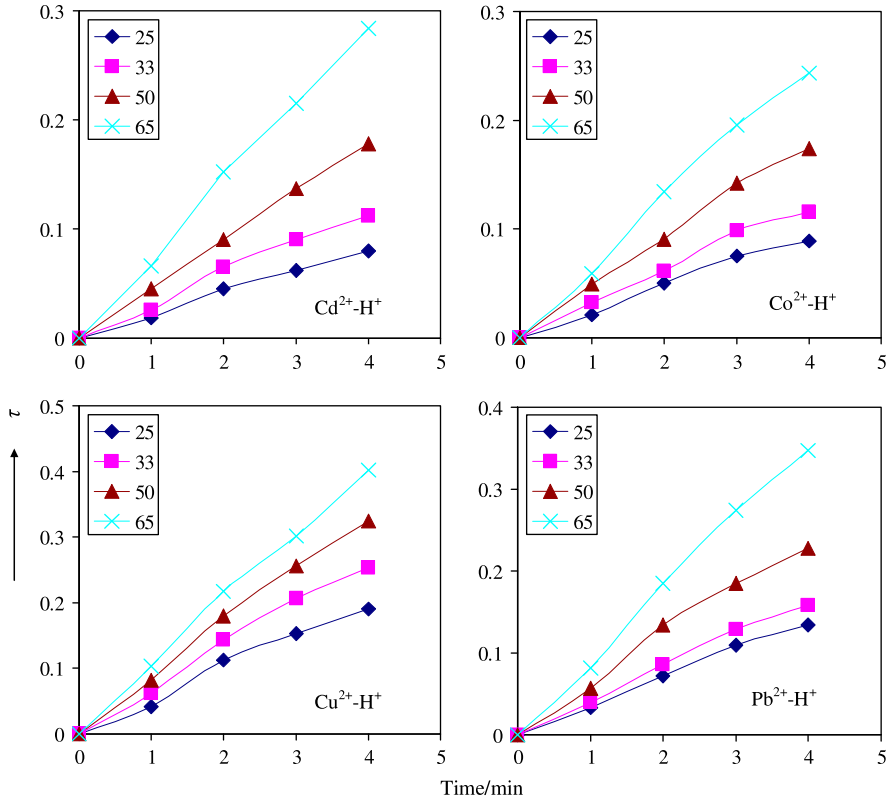


Fig. 4. Plots of $\tau$ vs. $t$ (time) for $Cd^{2+}$–$H^+$, $Co^{2+}$–$H^+$, $Cu^{2+}$–$H^+$, and $Pb^{2+}$–$H^+$ exchanges at different temperatures on acetonitrile stannic(IV) selenite composite cation exchanger.

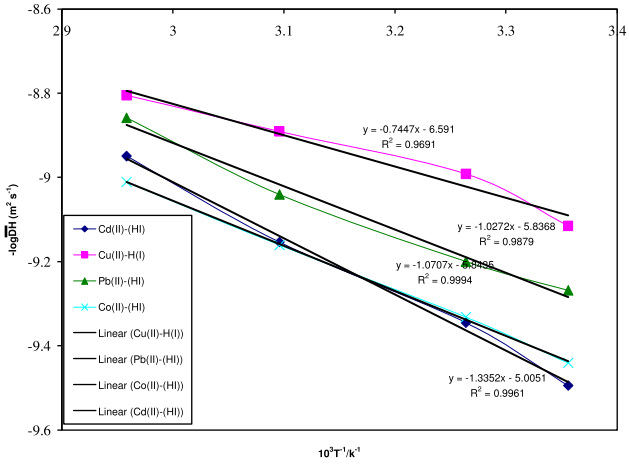


Fig. 5. Plots of $-\log \overline{D}_H$ vs. $10^3$ $T^{-1}/K^{-1}$ for $Cd^{2+}$–$H^+$, $Co^{2+}$–$H^+$, $Cu^{2+}$–$H^+$, and $Pb^{2+}$–$H^+$ exchanges on acetonitrile stannic(IV) selenite composite cation exchanger.

The pre-exponential constants $D_0$ are obtained by extrapolating these lines and using the intercepts at the origin. The activation energy ($E_a$) values are then calculated from the slope of plots. The entropy of activation ($\Delta S^*$) values were then calculated by substituting $D_o$ in Eq. (5).

$$D_0 = 2.72d^2(kT/h)\exp(\Delta S^*/R) \quad (5)$$

where $d$ is the ionic jump distance taken as $5 \times 10^{-10}$ m, $k$ is the Boltzmann constant, $R$ is the gas constant, $h$ is Planck's constant, and $T$ is taken as 273 K. The values of the diffusion coefficient ($D_o$), energy of activation ($E_a$), and entropy of activation ($\Delta S^*$) thus obtained are summarized in Table 2. The results showed that $D_0$, $E_a$, and $\Delta S^*$ are increasing as Cu<Co<Pb<Cd. The positive values of activation energy indicated that the minimum energy is required to facilitate the forward ($M^{2+}$–$H^+$) ion-exchange process. Negative values of the entropy of activation ($\Delta S^*$) suggest a greater degree of order achieved during the forward ion-exchange ($M^{2+}$–$H^+$) process. Higher values of coefficient for Cd(II) ions showed that the mobility of ions increased with respect to the activation energy required during forward ion-exchange process. The energies of activation shown was found higher as compared to other metal ions, which evident the separation capability of this cation-exchange material.

Table 1
Slopes of various τ vs. time (t) plots for $M^{2+}$–$H^+$ exchange processes on acetonitrile stannic(IV) selenite composite cation cation-exchanger at different temperatures

| Ion present in the ion exchanger | Migrating ions ⇓ Temperature ⇒ | $S$ ($s^{-1}$) | | | |
|---|---|---|---|---|---|
| | | 25℃ | 33℃ | 50℃ | 65℃ |
| $H^+$ | $Cd^{2+}$ | 0.0205 | 0.0289 | 0.0449 | 0.0719 |
| $H^+$ | $Cu^{2+}$ | 0.0491 | 0.0652 | 0.0823 | 0.1003 |
| $H^+$ | $Pb^{2+}$ | 0.0345 | 0.0404 | 0.0583 | 0.0887 |
| $H^+$ | $Co^{2+}$ | 0.0232 | 0.0298 | 0.0442 | 0.0624 |

Table 2
Values of $D_0$, $E_a$ and $\Delta S^*$ for the exchange of $H^+$ ions with some heavy toxic metal ions on acetonitrile stannic(IV) selenite composite cation-exchanger

| Ion present in the ion exchanger | Migrating ions | $D_0/m^2 s^{-1}$ | $E_a/kJ\ mol^{-1}$ | $\Delta S^*/J\ K^{-1}\ mol^{-1}$ |
|---|---|---|---|---|
| $H^+$ | $Cu^{2+}$ | $2.56 \times 10^{-7}$ | 0.7045 | −658.72 |
| $H^+$ | $Co^{2+}$ | $1.43 \times 10^{-6}$ | 1.0707 | −652.50 |
| $H^+$ | $Pb^{2+}$ | $1.46 \times 10^{-6}$ | 1.0749 | −651.06 |
| $H^+$ | $Cd^{2+}$ | $9.88 \times 10^{-6}$ | 1.3352 | −645.53 |

## 4. Conclusion

Kinetic studies revealed that the ion-exchange process is feasible over this composite cation-exchange material through particle diffusion controlled phenomenon. The fractional attainment of equilibrium $U(\tau)$ possessed corresponding values of ($\tau$) giving the straight lines passing through the origin, which are in accordance with the Nernst–Planck explicit approximation.

## Acknowledgement

This project was supported by King Saud University, Deanship of Scientific Research, College of Science Research Center.

### Abbreviation used

| | | |
|---|---|---|
| $U(\tau)$ | — | fractional attainment of equilibrium |
| $D_o$ | — | self diffusion coefficient |
| $E_a$ | — | energy of activation |
| $\Delta S^*$ | — | entropy of activation |
| i.d. | — | internal diameter |
| DMW | — | demineralized water |
| EDTA | — | ethylene diamine terta acetic acid, disodium salt |
| $\overline{D}_{H^+}$ | — | inter diffusion coefficient of counter ion $H^+$ |
| $\overline{D}_{M^{2+}}$ | — | inter diffusion coefficient of counter ion $M^{2+}$ |
| $r_o$ | — | particle radius |
| $\alpha$ | — | mobility ratio |
| $Z_{H^+}/Z_{M^{2+}}$ | — | charge ratio |
| $\tau$ | — | a dimensionless time parameter |
| $H^+$ | — | hydrogen ion |
| $M^{2+}$ | — | metal ion |
| $S$ | — | slope |
| $D$ | — | the ionic jump distance |
| $K$ | — | the Boltzmann constant |
| $R$ | — | gas constant |
| $H$ | — | Planck's constant |
| $T$ | — | temperature |

## References

[1] Agency for Toxic Substances and Disease Registry (ATSDR), Toxicological Profile for Cobalt, US Department of Health and Human Services, Atlanta, GA, 2001.
[2] World Health Organization (WHO), Guidelines for Drinking Water Quality, Health Criteria and Other Supporting Information, vol. 2, 2nd ed., World Health Organization, Geneva, 1998.
[3] International Agency for Research on Cancer (IARC), Monographs on the Evaluation of Carcinogenic Risk to Humans: Chlorinated Drinking Water, Chlorination Byproducts, Some Other Halogenated Compounds, Cobalt and Cobalt Compounds, vol. 52, IARC, Lyon, 1991.
[4] G.L. Millhauser, Copper binding in the prion protein, Acc. Chem. Res. 37 (2004) 79–85.
[5] E. Gaggelli, H. Kozlowski, D. Valensin, G. Valensin, Copper homeostasis and neurodegenerative disorders (Alzheimer's, Prion, and Parkinson's diseases and

amyotrophic lateral sclerosis), Chem. Rev. 106 (2006) 1995–2044.
[6] X. Yu, S. Tong, M. Ge, L. Wu, J. Zuo, C. Cao, W. Song, Adsorption of heavy metal ions from aqueous solution by carboxylated cellulose nanocrystals, J. Environ. Sci. 25 (2013) 933–943.
[7] M. Naushad, Surfactant assisted nano-composite cation exchanger: Development, characterization and applications for the removal of toxic $Pb^{2+}$ from aqueous medium, Chem. Eng. J. 235 (2014) 100–108.
[8] Y. Zhou, S. Wang, K. Zhang, X. Jiang, Visual detection of copper(II) by azide- and alkyne-functionalized gold nanoparticles using click chemistry, Angew. Chem. Int. Ed. 47 (2008) 7454–7456.
[9] J. Zhang, L. Zhang, Y. Wei, J. Ma, S. Shuang, Z. Cai, C. Dong, A selectively fluorescein-based colorimetric probe for detecting copper(II) ion, Spectrochim. Acta Mol. Biomol. Spectros. 122 (2014) 731–736.
[10] J.P. Cornard, A. Caudron, J.C. Merlin, UV–visible and synchronous fluorescence spectroscopic investigations of the complexation of Al(III) with caffeic acid, in aqueous low acidic medium, Polyhedron 25 (2006) 2215–2222.
[11] A. Martín-Cameán, A. Jos, A. Calleja, F. Gil, A. Iglesias-Linares, E. Solano, A.M. Cameán, Development and validation of an inductively coupled plasma mass spectrometry (ICP-MS) method for the determination of cobalt, chromium, copper and nickel in oral mucosa cells, Microchem. J. 114 (2014) 73–79.
[12] Mu. Naushad, Z.A. ALOthman, M.R. Khan, S.M. Wabaidur, Removal of bromate from water using De-Acidite FF-IP resin and determination by ultra-performance liquid chromatography-tandem mass spectrometry, Clean - Soil, Air, Water 41 (2013) 528–533.
[13] C.K. de Andrade, V.E. dos Anjos, M.L. Felsner, Y.R. Torres, S.P. Quináia, Direct determination of Cd, Pb and Cr in honey by slurry sampling electrothermal atomic absorption spectrometry, Food Chem. 146 (2014) 166–173.
[14] H. Bagheri, A. Afkhami, M. Saber-Tehrani, H. Khoshsafar, Preparation and characterization of magnetic nanocomposite of Schiff base/silica/magnetite as a preconcentration phase for the trace determination of heavy metal ions in water, food and biological samples using atomic absorption spectrometry, Talanta 97 (2012) 87–95.
[15] P. Chen, Y. Deng, K. Guo, X. Jiang, C. Zheng, X. Hou, Flow injection hydride generation for on-atomizer trapping: Highly sensitive determination of cadmium by tungsten coil atomic absorption spectrometry, Microchem. J. 112 (2014) 7–12.
[16] J.L. Guzmán-Mar, L. Hinojosa-Reyes, A.M. Serra, A. Hernández-Ramírez, V. Cerdà, Applicability of multisyringe chromatography coupled to cold-vapor atomic fluorescence spectrometry for mercury speciation analysis, Anal. Chim. Acta 708 (2011) 11–18.
[17] B. Feist, B. Mikula, Preconcentration of heavy metals on activated carbon and their determination in fruits by inductively coupled plasma optical emission spectrometry, Food Chem. 147 (2014) 302–306.
[18] Mu. Naushad, Z.A. ALOthman, M.R. Khan, Removal of malathion from aqueous solution using De-Acidite FF-IP resin and determination by UPLC–MS/MS: Equilibrium, kinetics and thermodynamics studies, Talanta 115 (2013) 15–23.
[19] V. Yilmaz, Z. Arslan, O. Hazer, H. Yilmaz, Selective solid phase extraction of copper using a new Cu(II)-imprinted polymer and determination by inductively coupled plasma optical emission spectroscopy (ICP-OES), Microchem. J. 114 (2014) 65–72.
[20] S. Arpadjan, G. Çelik, S. Taşkesen, S. Güçer, Arsenic, cadmium and lead in medicinal herbs and their fractionation, Food Chem. Toxicol. 46 (2008) 2871–2875.
[21] Mu. Naushad, A new ion-selective electrode based on aluminium tungstate for Fe(III) determination in rock sample, pharmaceutical sample and water sample, Bull. Mat. Sci. 31 (2008) 957–965.
[22] L. Zhao, S. Zhong, K. Fang, Z. Qian, J. Chen, Determination of cadmium(II), cobalt(II), nickel(II), lead(II), zinc(II), and copper(II) in water samples using dual-cloud point extraction and inductively coupled plasma optical emission spectrometry, J. Hazard. Mater. 206 (2012) 239–240.
[23] L. Zhu, L. Xu, B. Huang, N. Jia, L. Tan, S. Yao, Simultaneous determination of Cd(II) and Pb(II) using square wave anodic stripping voltammetry at a gold nanoparticle-graphene-cysteine composite modified bismuth film electrode, Electrochim. Acta 115 (2014) 471–477.
[24] K.M.L. Taylor-Pashow, T.C. Shehee, D.T. Hobbs, Advances in inorganic and hybrid ion exchangers, Solvent Ext. Ion Exc. 31 (2013) 122–170.
[25] Z.A. ALOthman, Inamuddin, Mu. Naushad, Recent developments in the synthesis, characterization and applications of zirconium(IV) based composite ion exchangers, J. Inorg. Organomet. Polym. 23 (2013) 257–269.
[26] Z.A. ALOthman, Inamuddin, Mu. Naushad, Forward ($M2^{+}-H^{+}$) and reverse ($H^{+}-M2^{+}$) ion exchange kinetics of the heavy metals on polyaniline Ce(IV) molybdate: A simple practical approach for the determination of regeneration and separation capability of ion exchanger, Chem. Eng. J. 171 (2011) 456–463.
[27] Mu. Naushad, A mercury ion selective electrode based on poly-*o*-toluidine Zr(IV) tungstate composite membrane, J. Electroanal. Chem. 713 (2014) 125–130.
[28] M.M.A. Khan, Rafiuddin, Inamuddin, PVC based polyvinyl alcohol zinc oxide composite membrane: Synthesis and electrochemical characterization for heavy metal ions, J. Ind. Eng. Chem. 19 (2013) 1365–1370.
[29] M.M. Alam, Z.A. ALOthman, M. Naushad, T. Aouak, Evaluation of heavy metal kinetics through pyridine based Th(IV) phosphate composite cation exchanger using particle diffusion controlled ion exchange phenomenon, J. Ind. Eng. Chem. 20 (2014) 705–709.
[30] Z.A. Al-Othman, Mu Naushad, A. Nilchi, Development, characterization and ion exchange thermodynamics for a new crystalline composite cation exchange material: Application for the removal of $Pb^{2+}$ ion from a standard sample (rompin hematite), J. Inorg. Organomet. Polym. 21 (2011) 547–559.
[31] M.J. Shaw, P.N. Nesterenko, G.W. Dicinoski, P.R. Haddad, Selectivity behaviour of a bonded phosphonate–carboxylate polymeric ion exchanger for metal cations with varying eluent compositions, J. Chromatog. A 997 (2003) 3–11.

[32] L.A. Attar, B. Safia, Sorption of $^{226}Ra$ from oil effluents onto synthetic cation exchangers, J. Environ. Manage. 124 (2013) 156–164.
[33] S.A. Nabi, R. Bushra, Z.A. Al-Othman, M. Naushad, Synthesis, characterization, and analytical applications of a new composite cation exchange material acetonitrile stannic(IV) selenite: Adsorption behavior of toxic metal ions in nonionic surfactant medium, Sep. Sci. Technol. 46 (2011) 847–857.
[34] C.N. Reilley, R.W. Schmid, F.S. Sadek, Chelon approach to analysis: I. Survey of theory and application, J. Chem. Edu. 36 (1959) 555–565.
[35] F. Helfferich, M.S. Plesset, Ion exchange kinetics: A nonlinear diffusion problem, office of naval research department of navy contract No. 220(28), Report No. 85–87, 1957.
[36] S. Kodama, K. Fukui, A. Mazume, Relation of space velocity and space time yield, Ind. Eng. Chem. 45 (1953) 1644–1648.
[37] F. Helfferich, M.S. Plesset, Ion exchange kinetics: A nonlinear diffusion problem, J. Chem. Phys. 28 (1958) 418–424.
[38] M.S. Plesset, F. Helfferich, J.N. Franklin, Ion exchange kinetics: A nonlinear diffusion problem. II. Particle diffusion controlled exchange of univalent and bivalent ions, J. Chem. Phys. 29 (1958) 1064–1069.
[39] F. Helfferich, Ion Exchange, McGraw-Hill, New York, NY, 1962 (Chapter 3).